Fluid Mechanics
2016; 2(1): 1-7
http://www.sciencepublishinggroup.com/j/fm
doi: 10.11648/j.fm.20160201.11

Axisymmetric Stagnation Flow of a Micropolar Fluid in a Moving Cylinder: An Analytical Solution

Abdul Rehman[1, *], Saleem Iqbal[1], Syed Mohsin Raza[2]

[1]Department of Mathematics, University of Balochistan, Quetta, Pakistan

[2]Department of Physics, University of Balochistan, Quetta, Pakistan

Email address:
rehman_maths@hotmail.com (A. Rehman)
[*]Corresponding author

To cite this article:
Abdul Rehman, Saleem Iqbal, Syed Mohsin Raza. Axisymmetric Stagnation Flow of a Micropolar Fluid in a Moving Cylinder: An Analytical Solution. *Fluid Mechanics*. Vol. 2, No. 1, 2016, pp. 1-7. doi: 10.11648/j.fm.20160201.11

Received: July 12, 2016; **Accepted**: July 22, 2016; **Published**: August 26, 2016

Abstract: In this paper, we have presented the axisymmetric stagnation flow of a micropolar fluid in a moving cylinder. The governing equations of motion, microrotation and energy are simplified with the help of suitable similarity transformations. System of six nonlinear coupled differential equations has been solved analytically with the help of strong analytical tool known as homotopy analysis method. The physical features of various parameters have been discussed through graphs.

Keywords: Series Solution, Axisymmetric Stagnation Flow, Micropolar Fluid, Moving Cylinder

1. Introduction

Numerous applications of stagnation flows in engineering and scientific interest have attracted the attention of number of researchers [1-5]. In some situations flow is stagnated by a solid wall, while in others a free stagnation point or line exist interior to the fluid domain [6]. The stagnation point flows can be viscous or inviscid, steady or unsteady, two dimensional or three dimensional, normal or oblique and forward or reverse. The stagnation flows were initiated by Hiemenz [7] and Homann [8]. Recently, Hong and Wang [9] have discussed the annular axisymmetric stagnation flow on a moving cylinder. According to Hong and Wang [9], in the previous literature the researchers have considered a stagnation flow originated from infinity. But there are certain situations in which finite geometry is more realistic and attractive for high speed and miniature rotating systems [10, 11].

In the situations like polymeric fluids or certain naturally occurring fluids such as blood, the classical Navier Stokes theory does not hold [22]. Therefore, Erigen [23] has given the idea of micropolar fluid which describes both the effect of couple stresses and the microscopic effects arising from local structure and microrotation of the fluid elements. Also, the micropolar fluids consist of a suspension of small, rigid, cylindrical elements such as large dumbbell shaped molecules. Erigen [24] has also developed the theory of thermomicropolar fluids by extending the theory of micropolar fluids. Because of importance of this theory a large amount of literature on micropolar fluids with different geometries are now available. Few of them are cited in the Ref [25-27].

Motivated from the above highlights, the purpose of the present work is to extend the idea of Hong and Wang [9] for micropolar fluid. To the best of author's knowledge, not a single article is available in literature which discusses the axisymmetric stagnation flow of non-Newtonian fluid with a finite geometry. The problem has been first simplified with the help of suitable similarity transformations and then solved with the analytical technique known as homotopy analysis method (HAM), some relevant work on HAM are given in the Ref [28-34]. The convergence of the HAM solution has been discussed through $\hbar$ -curves. A comparison of our HAM solution and previous numerical solutions for viscous fluid is also presented. At the end, the physical behavior of pertinent parameters is discussed through graphs. Few important works concerning fluid flow through cylindrical geometry are cited in [36-40].

2. Formulation

Let us consider an incompressible flow of a micropolar fluid between two cylinders. We are considering cylindrical geometry assuming that the flow is axisymmetric about z-axis. The inner cylinder is of radius R rotating with angular velocity Ω and moving with velocity W in the axial z-direction. The inner cylinder is enclosed by an outer cylinder of radius bR. The fluid is injected radially with velocity U from the outer cylinder towards the inner cylinder. The equations for micropolar fluid in the presence of heat transfer analysis are stated as

$$rw_z + (ru)_r = 0, \quad (1)$$

$$\rho(uu_r + wu_z - \frac{v^2}{r}) = -p_r + (\mu + k)(u_{rr} + \frac{1}{r}u_r + u_{zz} - \frac{u}{r^2}) - kN_z^*, \quad (2)$$

$$\rho\left(uv_r + wv_z + \frac{uv}{r}\right) = (\mu + k)(v_{rr} + \frac{1}{r}v_r + v_{zz} - \frac{v}{r^2}), \quad (3)$$

$$\rho(uw_r + ww_z) = -p_z + (\mu + k)(w_{rr} + \frac{1}{r}w_r + w_{zz}) + k\left(N_r^* + \frac{1}{r}N^*\right) \quad (4)$$

$$\rho j\left(uN_r^* + wN_z^*\right) = -2kN^* + k(u_z - w_r) + \gamma\left(N_{rr}^* + \frac{1}{r}N_r^* + N_{zz}^* - \frac{1}{r^2}N^*\right), \quad (5)$$

$$c_p(uT_r + wT_z) = \frac{k^*}{\rho}(T_{rr} + \frac{1}{r}T_r + T_{zz}), \quad (6)$$

where (u, v, w) are the velocity components along the (r, θ, z) directions, N^* is the angular microrotation momentum, μ is the dynamic viscosity, k is the vertex viscosity, ρ is the density, j is the microrotation density, γ is the micropolar constant, c_p is the specific heat at constant pressure, T is the temperature, v is the kinematic viscosity, k^* is the thermal conductivity and p is the pressure.

Defining the following similarity transformations and non-dimensional variables

$$u = -\frac{Uf(\eta)}{\sqrt{\eta}}, v = \Omega a h(\eta), w = 2Uf'(\eta)\xi + Wg(\eta), \quad (7)$$

$$N^* = 2\frac{U}{R}M(\eta)\xi + \frac{W}{R}N(\eta),\ \theta = \frac{T - T_1}{T_b - T_1}, \quad (8)$$

$$\eta = \frac{r^2}{R^2} \quad \xi = \frac{z}{R}. \quad (9)$$

With the help of these above transformations, $Eq.(1)$ is identically satisfied and $Eqs.(2)$ to (6) take the following form

$$\eta f^{(IV)} + 2f''' + \frac{\mathrm{Re}}{1+K}(ff''' - ff'') + \frac{K}{8(1+K)\sqrt{\eta}}\left(4\eta M'' + 4M' - \frac{M}{\eta}\right) = 0, \quad (10)$$

$$\eta g'' + g' + \frac{\mathrm{Re}}{(1+K)}(fg' - f'g) + \frac{K}{(1+K)}\sqrt{\eta}\left(4N' + \frac{2N}{\eta}\right) = 0, \quad (11)$$

$$4\eta h'' + 4h' - \frac{h}{\eta} + \frac{\mathrm{Re}}{(1+K)}\left(4fh' + \frac{2fh}{\eta}\right) = 0, \quad (12)$$

$$4\eta M'' + 4M' - \frac{M}{\eta} - \frac{4\mathrm{Re}}{\Lambda}(fM' + f'M) - \frac{2K\delta}{\Lambda}\left(M + \sqrt{\eta}f''\right) = 0, \quad (13)$$

$$4\eta N'' + 4N' - \frac{N}{\eta} - \frac{4\mathrm{Re}}{\Lambda}(fN' + Mg) - \frac{2K\delta}{\Lambda}\left(N + \sqrt{\eta}g'\right) = 0, \quad (14)$$

$$\eta\theta'' + \theta' + \mathrm{Pr}\,\mathrm{Re}\, f\theta' = 0, \quad (15)$$

in which $\mathrm{Re} = UR/2\nu$ is the cross-flow Reynolds number, $K = k/\mu$ is the micropolar parameter, $\Lambda = \gamma/\mu j$ and $\delta = R^2/j$ are the micropolar coefficients and $\mathrm{Pr} = \nu\rho c_p / k^*$ is the Prandtl number.

The boundary conditions in nondimentional form are defined as

$$f(1) = 0, f'(1) = 0, f(b) = \sqrt{b}, f'(b) = 0, \theta(1) = 0, \quad (16)$$

$$g(1) = 1,\ g(b) = 0,\ h(1) = 1,\ h(b) = 0,\ \theta(b) = 1, \quad (17)$$

$$M(1) = -2nf''(1),\ M(b) = 0,\ N(1) = -2ng'(1),\ N(b) = 0 \quad (18)$$

3. Solution of the Problem

The solution of the above boundary value problem is obtained with the help of HAM. For HAM solution, we choose the initial guesses as

$$f_0(\eta) = \frac{\sqrt{b}}{b-1}((3b-1) - 6b\eta + 3(b+1)\eta^2 - 2\eta^3, \quad (19)$$

$$g_0(\eta) = \frac{b-\eta}{b-1},\ h_0(\eta) = \frac{b-\eta}{b-1}, \quad (20)$$

$$M_0(\eta) = \frac{-6\sqrt{b}n}{(b-1)^3}(b-\eta),\ N_0(\eta) = \frac{2n}{(b-1)^2}(b-\eta),\ \theta_0(\eta) = \frac{\eta-1}{b-1}, \quad (21)$$

with the corresponding auxiliary linear operators

$$L_f = \frac{d^4}{d\eta^4},\ L_g = \frac{d^2}{d\eta^2},\ L_h = \frac{d^2}{d\eta^2}, \quad (22)$$

$$L_M = \frac{d^2}{d\eta^2},\ L_N = \frac{d^2}{d\eta^2},\ L_\theta = \frac{d^2}{d\eta^2}, \quad (23)$$

satisfying

$$L_f[c_1 + c_2\eta + c_3\eta^2 + c_4\eta^3] = 0, \quad (24)$$

$$L_g[c_5 + c_6\eta] = 0,\ L_h[c_7 + c_8\eta] = 0, \quad (25)$$

$$L_M[c_9+c_{10}\eta]=0,\ L_N[c_{11}+c_{12}\eta]=0,\ L_\theta[c_{13}+c_{14}\eta]=0, \quad (26)$$

where $c_i\left(i=1,...,14\right)$ are arbitrary constants. The zeroth-order deformation equations are defined as

$$\left(1-p\right)L_f[\hat{f}\left(\eta;p\right)-f_0\left(\eta\right)]=p\hbar_1N_f[\hat{f}\left(\eta;p\right)], \quad (27)$$

$$\left(1-p\right)L_g[\hat{g}\left(\eta;p\right)-g_0\left(\eta\right)]=p\hbar_2N_g[\hat{g}\left(\eta;p\right)], \quad (28)$$

$$\left(1-p\right)L_h[\hat{h}\left(\eta;p\right)-h_0\left(\eta\right)]=p\hbar_3N_h[\hat{h}\left(\eta;p\right)], \quad (29)$$

$$\left(1-p\right)L_M[\hat{M}\left(\eta;p\right)-M_0\left(\eta\right)]=p\hbar_4N_M[\hat{M}\left(\eta;p\right)], \quad (30)$$

$$\left(1-p\right)L_N[\hat{N}\left(\eta;p\right)-N_0\left(\eta\right)]=p\hbar_5N_N[\hat{N}\left(\eta;p\right)], \quad (31)$$

$$\left(1-p\right)L_\theta[\hat{\theta}\left(\eta;p\right)-\theta_0\left(\eta\right)]=p\hbar_6N_\theta[\hat{\theta}\left(\eta;p\right)], \quad (32)$$

where

$$N_f[\hat{f}\left(\eta;p\right)]=\eta\hat{f}^{iv}+2\hat{f}'''+\frac{\mathrm{Re}}{1+K}(\hat{f}\hat{f}'''-\hat{f}'\hat{f}'')+\frac{K}{8\left(1+K\right)\sqrt{\eta}}\left(4\eta\hat{M}''+4\hat{M}'-\frac{\hat{M}}{\eta}\right), \quad (33)$$

$$N_g[\hat{g}\left(\eta;p\right)]=\eta\hat{g}''+\hat{g}'+\frac{\mathrm{Re}}{\left(1+K\right)}\left(\hat{f}\hat{g}'-\hat{f}'\hat{g}\right)+\frac{K}{\left(1+K\right)}\sqrt{\eta}\left(4\hat{N}'+\frac{2\hat{N}}{\eta}\right), \quad (34)$$

$$N_h[\hat{h}\left(\eta;p\right)]=4\eta\hat{h}''+4\hat{h}'-\frac{\hat{h}}{\eta}+\frac{\mathrm{Re}}{\left(1+K\right)}\left(4\hat{f}\hat{h}'+\frac{2\hat{f}\hat{h}}{\eta}\right), \quad (35)$$

$$N_M[\hat{M}\left(\eta;p\right)]=4\eta\hat{M}''+4\hat{M}'-\frac{\hat{M}}{\eta}-\frac{4\,\mathrm{Re}}{\Lambda}(\hat{f}\hat{M}'+\hat{f}'\hat{M})-\frac{2K\delta}{\Lambda}\left(\hat{M}+\sqrt{\eta}\hat{f}''\right), \quad (36)$$

$$N_N[\hat{N}\left(\eta;p\right)]=4\eta\hat{N}''+4\hat{N}'-\frac{\hat{N}}{\eta}-\frac{4\,\mathrm{Re}}{\Lambda}\left(\hat{f}\hat{N}'+\hat{M}\hat{g}\right)-\frac{2K\delta}{\Lambda}\left(\hat{N}+\sqrt{\eta}\hat{g}'\right), \quad (37)$$

$$N_\theta[\hat{\theta}\left(\eta;p\right)]=\eta\hat{\theta}''+\hat{\theta}'+\mathrm{Pr}\,\mathrm{Re}\,\hat{f}\hat{\theta}'. \quad (38)$$

The boundary conditions for the zeroth order system are

$$\hat{f}\left(1;p\right)=0,\ \hat{f}'\left(1;p\right)=0,\ \hat{g}\left(1;p\right)=1,\ \hat{h}\left(1;p\right)=1,\ \hat{\theta}\left(1;p\right)=0, \quad (39)$$

$$\hat{f}\left(b;p\right)=\sqrt{b},\ \hat{f}'\left(b;p\right)=0,\ \hat{g}\left(b;p\right)=0,\ \hat{h}\left(b;p\right)=0,\ \hat{\theta}\left(b;p\right)=1, \quad (40)$$

$$\hat{M}\left(1;p\right)=-2nf_0''\left(1\right),\ \hat{M}\left(b;p\right)=0,\ \hat{N}\left(1;p\right)=2ng_0'\left(1\right),\ \hat{N}\left(b;p\right)=0, \quad (41)$$

The m^{th} order deformation equations can be obtained by differentiating the zeroth-order deformation equations $\left(27-32\right)$ and the boundary conditions $(39-41)$, m- times with respect to p, then dividing by $m!$, and finally setting $p=0$, we get

$$L_f[f_m\left(\eta\right)-\chi_mf_{m-1}\left(\eta\right)]=\hbar_1R_{mf}\left(\eta\right), \quad (42)$$

$$L_g[g_m\left(\eta\right)-\chi_mg_{m-1}\left(\eta\right)]=\hbar_2R_{mg}\left(\eta\right), \quad (43)$$

$$L_h[h_m\left(\eta\right)-\chi_mh_{m-1}\left(\eta\right)]=\hbar_3R_{mh}\left(\eta\right), \quad (44)$$

$$L_M[M_m\left(\eta\right)-\chi_mM_{m-1}\left(\eta\right)]=\hbar_4R_{mM}\left(\eta\right), \quad (45)$$

$$L_N[N_m\left(\eta\right)-\chi_mN_{m-1}\left(\eta\right)]=\hbar_5R_{mN}\left(\eta\right), \quad (46)$$

$$L_\theta[\theta_m\left(\eta\right)-\chi_m\theta_{m-1}\left(\eta\right)]=\hbar_6R_{m\theta}\left(\eta\right), \quad (47)$$

$$f_m\left(1\right)=0,\ f_m'\left(1\right)=0,\ g_m\left(1\right)=0,\ h_m\left(1\right)=0,\ \theta_m\left(1\right)=0, \quad (48)$$

$$f_m\left(b\right)=0,\ f_m'\left(b\right)=0,\ g_m\left(b\right)=0,\ h_m\left(b\right)=0,\ \theta_m\left(b\right)=0, \quad (49)$$

$$M_m\left(1\right)=0,\ M_m\left(b\right)=0,\ N_m\left(1\right)=0,\ N_m\left(b\right)=0, \quad (50)$$

Further details of the HAM solution are presented in the next section.

4. Results and Discussion

The HAM solutions for the differential system are heavily dependent upon the selection of involved auxiliary parameters for the respective profiles. *Figures* 1 and 2 contain $\hbar$ curves for the convergence regions of different velocity profiles at the surface of the inner cylinder. *Figure* 1 shows the $\hbar$ curves for the linear velocity profiles f and h for specified values of the involved parameters. It is noticed from *Figure* 1 that the convergence region for f' is the least. *Figure* 2 shows the convergence region for linear velocity profile g and angular velocity profiles M and N for presented values of the other parameters. From *Figure* 2 it is noted that the convergence region for angular velocity profiles is much larger than that for linear velocity profiles. From *Figure* 2 it is also observed that the suitable choice of auxiliary convergence parameter $\hbar_2$ for the nondimensional linear velocity profile g is $-0.9\le\hbar_2\le-0.2$. *Figure* 3 tweets the influence of Reynolds numbers Re over the linear velocity and acceleration profiles f, g and f' for specified values of the involved parameters. *Figure* 3 dictates that with increase in Reynolds numbers Re, the nondimensional linear velocity profile f increases, while g decreases, whereas the nondimensional acceleration profile f' has shown dual behavior that is near the surface of inner cylinder the acceleration profile f' increases, f' has a turning point somewhere $\eta = \sqrt{2}$ and in the neighborhood of outer cylinder the acceleration profile decreases. *Figure* 4 predicts the influence of the micropolar parameter K over the velocity and acceleration profiles f, h and f'. It is observed from *Figure* 4 that with increase in K, the nondimensional velocity profile f increases while h decreases, whereas the nondimensional acceleration profile has dual behavior that is f' decreases near the surface of the inner cylinder while near the surface of the outer cylinder the nondimensional acceleration profile f' increases. *Figures* $5a$ and $5b$ gives the behavior of linear velocity profiles g and h for different values of the micropolar parameter K and the Reynolds numbers Re respectively. From these sketches it is evident that both velocity profiles g and h exhibits decreasing behavior with respect to the specified parameters. The influence of micropolar parameter K and micropolar coefficient Λ over the angular velocity profile M are presented in *Figures* $6a$ and $6b$ for the case of weak concentration with $n = 1/2$. From these plates it is observed that with respect to both micropolar parameter K and micropolar coefficient Λ the micropolar velocity profile M decreases. The effects of micropolar parameter K and micropolar coefficient Λ over the microrotation profile N are portrayed in *Figures* $7a$ and $7b$ respectively. It is seen from *Figures* $7a$ and $7b$ that with increase in micropolar parameter K, the microrotaion profile N increases, while with increase in micropolar coefficient Λ, the microrotaion profile N decreases. The influence of micropolar parameter K over micropolar velocites M and N for the case of strong concentration with $n = 0$ is presented in *Figures* $8a$ and $8b$ respectively. The observed behavior indicates that the micropolar velocity M has a sinusoidal behavior while N exhibits increasing influence. The influence of Prandtl numbers Pr and Reynolds numbers Re over the temperature profile θ is presented in *Figures* $9a$ and $9b$. From these figures it is observed that with increase in both Prandtl numbers Pr and Reynolds numbers Re the temperature profile increases.

A comparison of our HAM solutions with the available numerical solutions in [9] without microrotation effects are shown in *Table 1*. It is seen that both solutions are almost identical. The value of skinfriction coefficient is presented in Table. 2. It is seen that with the increase in Re, the skinfriction coefficient decreases, however the magnitude of skinfriction increases with the increase in α.

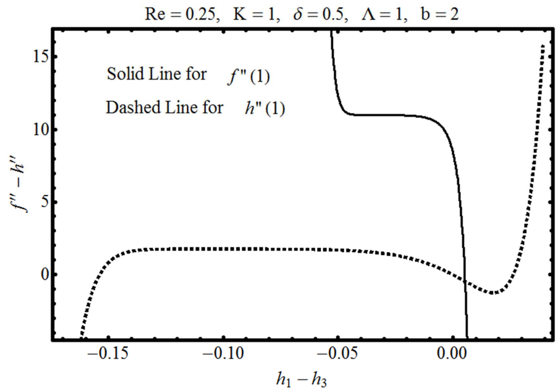

Figure 1. *ħ curves for velocity profiles* f *and* h .

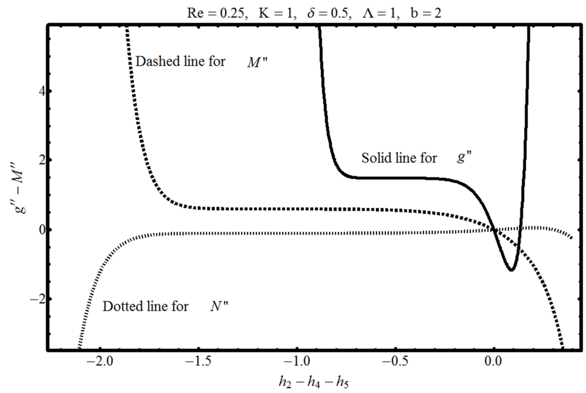

Figure 2. *ħ curves for velocity profile* g *and microrotation profiles* M *and* N .

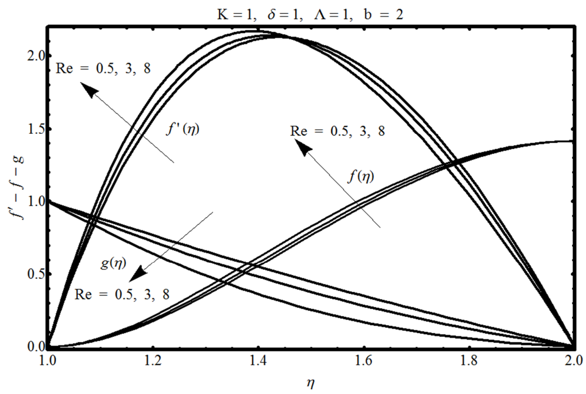

Figure 3. *Influence of* Re *over the velocity profiles* f, f' *and* g .

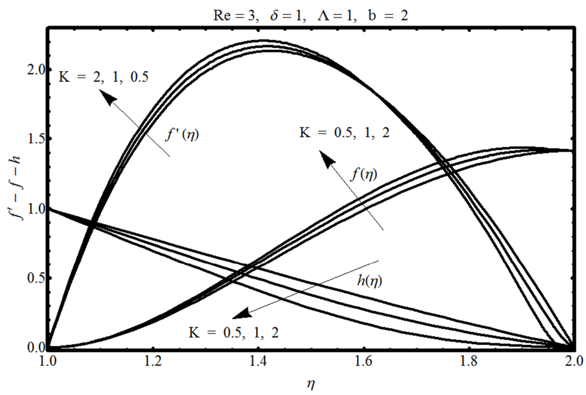

Figure 4. *Influence of* K *over the velocity profiles* f, f' *and* h .

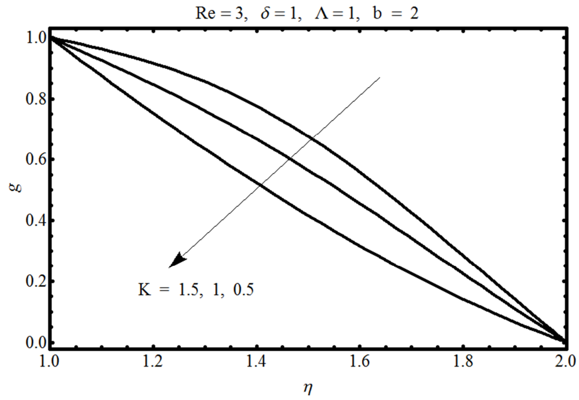

Figure 5a. *Influence of* K *over* g .

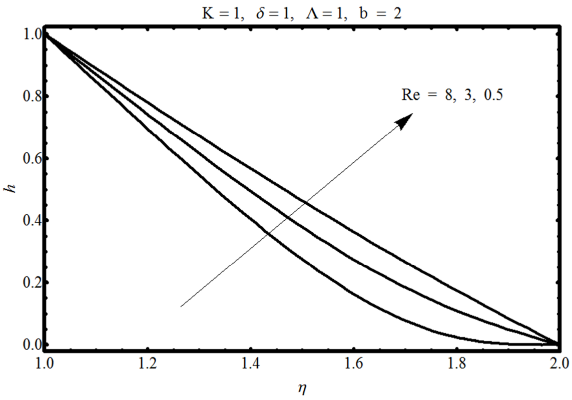

Figure 5b. *Influence of* Re *over* h .

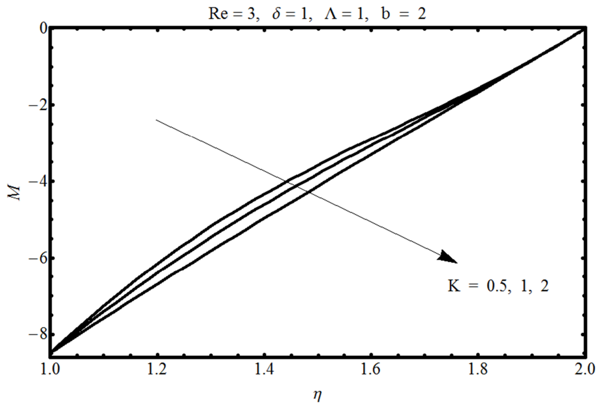

Figure 6a. *Influence of* K *over* M .

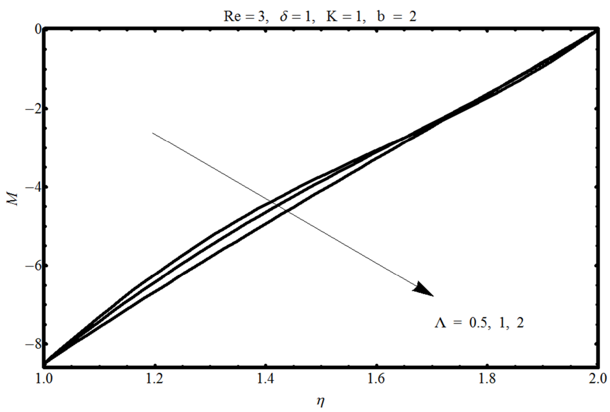

Figure 6b. *Influence of* Λ *over* M .

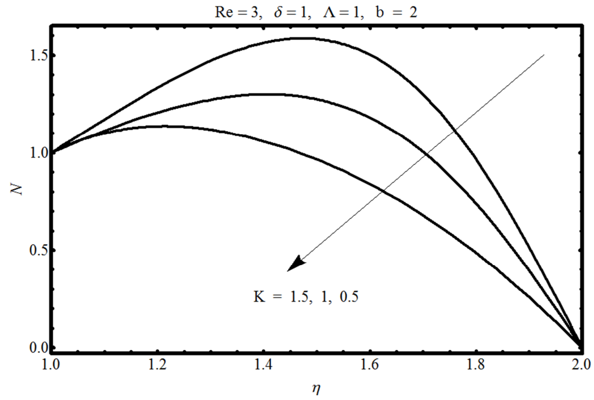

Figure 7a. *Influence of* K *over* N .

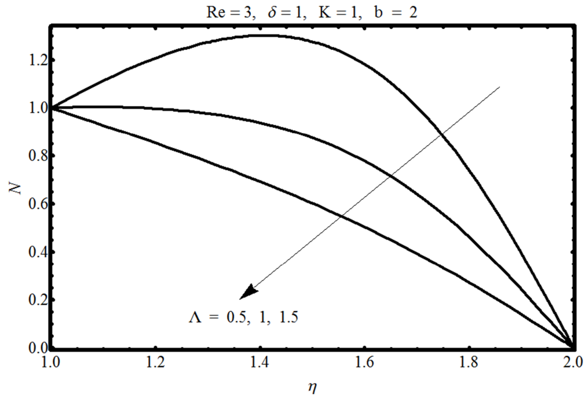

Figure 7b. *Influence of* Λ *over* N .

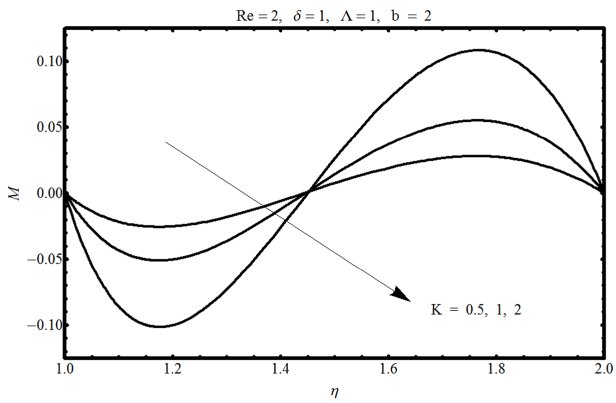

Figure 8a. *Influence of* K *over* M *for* $n = 0$.

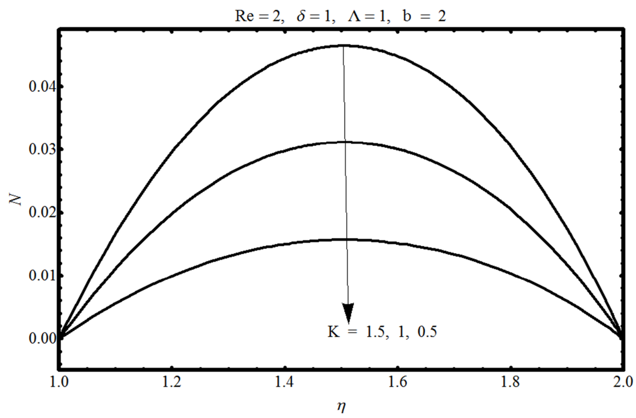

Figure 8b. *Influence of* K *over* N *for* $n = 0$.

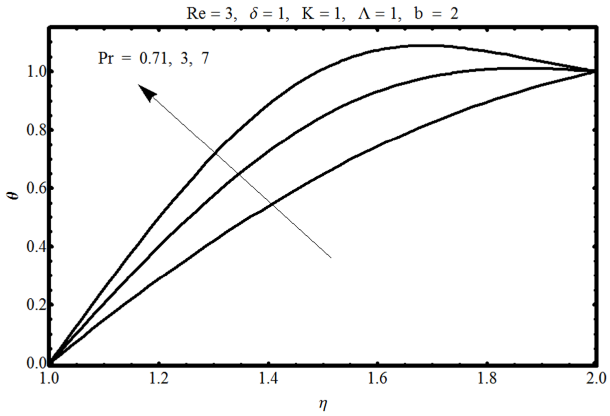

Figure 9a. *Influence of* Pr *over the temperature profile* θ .

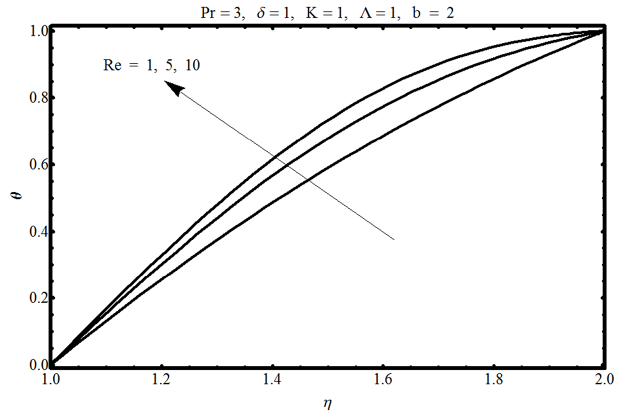

Figure 9b. *Influence of* Re *over the temperature profile* θ .

Table 1. *Comparison of boundary derivatives of present results with the available work of [9].*

Re\b	**1.1**		**2**		**10**	
	[9]	**Present**	**[9]**	**Present**	**[9]**	**Present**
f´´(1)						
0.1	650.3526	650.3526	11.0010	11.0010	0.667	0.667
1	654.7679	654.7679	11.6772	11.6772	0.863	0.863
10	698.6176	698.6176	17.5348	17.5348	1.867	1.867
-f´´´(1)						
0.1	13883	13883	36.1443	36.1443	0.9172	0.9172
1	14117	14117	41.0797	41.0797	1.3924	1.3924
10	16507	16507	93.5670	93.5670	5.2400	5.2400
-g´(1)						
0.1	10.5382	10.5382	1.4963	1.4963	0.5082	0.5082
1	10.9489	10.9489	1.9309	1.9309	0.9040	0.9040
10	14.6586	14.6586	4.3856	4.3856	2.2168	2.2168
-h´(1)						
0.1	10.5151	10.5151	1.5151	1.5151	0.6235	0.6235
1	10.6511	10.6511	1.6554	1.6554	0.7570	0.7570
10	12.0407	12.0407	3.0517	3.0517	1.5941	1.5941

Table 2. *Variation of skin friction coefficient for different values of Re/α.*

	K = 0, n = 0, ξ = 1			**K = 1, n = 1/2, ξ = 1**			**K = 3, n = 1/2, ξ = 1**		
Re\α	**0**	**1**	**2**	**0**	**1**	**2**	**0**	**1**	**2**
0.1	353.767	412.605	389.131	432.517	-806.22	-2027.39	438.586	-2241.65	-2257.97
1	35.7919	43.1997	39.2168	44.6699	-1754.12	-3550.89	44.7221	-3167.30	-3154.96
5	7.52430	10.0520	9.37830	10.1557	-5764.42	-11538.4	9.70790	-6364.88	-6328.78
10	3.98710	8.35250	5.52620	5.77890	-13304.9	-26615.1	5.20750	-11903.3	-11820.3

References

[1] F. Labropulu and D. Lia, Stagnation-Point Flow of a Second-grade Fluid with Slip, Int J Non-Linear Mec, 43 (2008) 941-947.

[2] V. Kumaran, R. Tamizharasi and K. Vajravelu, Approximate Analytic Solutions of Stagnation Point Flow in a Porous Medium, Comm Nonlinear Sci Num Simu, 14 (2009) 2677-2688.

[3] C. Y. Wang, Axisymmetric Stagnation Flow on a Cylinder, Quart. Appl. Math, 32 (1974) 207-213.

[4] C. Y. Wang, Off-centered Stagnation Flow Towards a Rotating Disc, Int. J. Engag. Sci. 46 (2008) 391-396.

[5] C. Y. Wang, Stagnation Slip Flow and Heat Transfer on a Moving Plate, Che. Eng. Sci, 61 (2006) 7668-7672.

[6] F. Labropulu, D. Li and I. Pop, Non-orthogonal Stagnation-point Flow Towards a Stretching Surface in a non-Newtonian Fluid with Heat Transfer, Int. J. Ther. Sci, 49 (2010) 1042-1050.

[7] K. Hiemenz, Die Grenzschicht an Einem in den Gleichformingen Flussigkeitsstrom Eingetauchten graden Kreiszylinder, Dinglers Polytech. J. 326 (1911) 321-324.

[8] F. Homann, Der Einfluss grosser Zahighkeit bei der Stromung um den Zylinder und um die Kugel. Zeitschrift fur angewandte Mathematik und Mechanik 16 (1936) 153-164.

[9] L. Hong and C. Y. Wang, Annular Axisymmetric Stagnation Flow on a Moving Cylinder, Int. J. Engag. Sci. 47 (2009) 141-152.

[10] S. Heller, W. Shapiro and O. Decker, A Porous Hydrostatic gas Bearing for use in Miniature Turbomachinery, ASLE Trans. 22 (1971) 144-155.

[11] B. C. Majumdar, Analysis of Externally Pressurized Porous gas Bearings-1, Wear 33 (1975) 25-35.

[12] S. Nadeem, Abdul Rehman, K. Vajravelu, Jinho Lee, Changhoon Lee, Axisymmetric stagnation flow of a micropolar nanofluid in a moving cylinder, Mathematical Problems in Engineering, Volume 2012, Article ID 378259.

[13] S. Nadeem, Abdul Rehman, Axisymmetric stagnation flow of a nanofluid in a moving cylinder, Comp. Math. Mod. 24 (2) (2013) 293-306.

[14] Abdul Rehman, S. Nadeem, M. Y. Malik, Stagnation flow of couple stress nanofluid over an exponentially stretching sheet through a porous medium, J. Power Tech. 93 (2) (2013) 122-132.

[15] Abdul Rehman, S. Nadeem, Heat transfer analysis of the boundary layer flow over a vertical exponentially stretching cylinder, Global J. Sci. Fron. Res. 13 (11) (2013) 73-85.

[16] M. Y. Malik, M. Naseer, S. Nadeem, Abdul Rehman, The boundary layer flow of Casson nanofluid over a vertical exponentially stretching cylinder, Appl. NanoSci. DOI: 10.1007/s13204-012-0267-0.

[17] Abdul Rehmana, S. Achakzai, S. Nadeem, S. Iqbal, Stagnation point flow of Eyring Powell fluid in a vertical cylinder with heat transfer, Journal of Power Technologies 96 (1) (2016) 57–62

[18] Abdul Rehman, S. Nadeem, S. Iqbal, M. Y. Malik, M. Naseer, Nanoparticle effect over the boundary layer flow over an exponentially stretching cylinder, J. NanoEngineering and NanoSystems (2014) 1-6.

[19] Abdul Rehman, G. Farooq, I. Ahmed, M. Naseer, M. Zulfiqar, Boundary Layer Stagnation-Point Flow of Second Grade Fluid over an Exponentially Stretching Sheet, American J App Math Stat, 3 (6) (2015) 211-219.

[20] M. Y. Malik, M. Naseer, S. Nadeem, Abdul Rehman, The boundary layer flow of huperbolic tangent fluid over a vertical exponentially stretching cylinder, Alexandria Eng. J., 53 (2014) 747-750.

[21] M. Y. Malik, M. Naseer, Abdul Rehman, Numerical study of convective heat transfer on the Power Law fluid over a vertical exponentially stretching cylinder, App Comp Math, 4 (5), (2015) 346-350.

[22] A. C. Eringen, Theory of Micropolar Fluids, J. Math. Mech. 16 (1966) 1-18.

[23] Chun-I Chen, Non-linear Stability Characterization of the Thin Micropolar Liquid Film Flowing Down the Inner Surface of a Rotating Vertical Cylinder, Commun Nonlinear Sci Numer Simulat. 12 (2007) 760-775.

[24] S. Nadeem, Noreen Sher Akbar and M. Y. Malik, Exact and Numerical Solutions of a Micropolar Fluid in a Vertical Annulus, Wiley InterScience, DOI 10.1002/num.20517.

[25] R. Nazar and N. Amin, Free Convection Boundary Layer on an Isothermal Sphere in a Micropolar Fluid, Int Comm Heat Mass Tran, 29 (2002) 377-386.

[26] R. Nazar, N. Amin, T. Gro and I. Pop, Free Convection Boundary Layer on a Sphere with Constant Surface Heat Flux in a Micropolar Fluid, Int Comm Heat Mass Tran, 29 (2002) 1129-1138.

[27] S. Nadeem, Abdul Rehman, Mohamed Ali, The boundary layer flow and heat transfer of a nanofluid over a vertical slender cylinder, J. NanoEngineering and NanoSystems (2012) 1-9.

[28] S. Abbasbandy, Soliton Solutions for the Fitzhugh-Nagumo Equation with the Homotopy Analysis Method, Appl. Math Mod 32 (2008) 2706-2714.

[29] Abdul Rehman, S. Nadeem, M. Y. Malik, Boundary layer stagnation-point flow of a third grade fluid over an exponentially stretching sheet, Braz. J. Che. Eng. 30 (3) (2013) 611-618.

[30] Sj. Liao, Beyond Perturbation: Introduction to the Homotopy Analysis Method, Chapman & Hall/CRC Press, Boca Raton (2003).

[31] S. Nadeem, Anwar Hussain and Majid Khan, HAM Solutions for Boundary Layer Flow in the Region of the Stagnation Point Towards a Stretching Sheet, Commun Nonlinear Sci Numer Simulat. 15 (2010) 475-481.

[32] S. Nadeem, Abdul Rehman, Changhoon Lee, Jinho Lee, Boundary layer flow of second grade fluid in a cylinder with heat transfer, Mathematical Problems in Engineering, Volume 2012, Article ID 640289.

[33] Sj. Liao, On the Homotopy Analysis Method for nonlinear Problems, Appl Math Comput 147/2 (2004) 499-513.

[34] Abdul Rehman, S. Nadeem, Mixed convection heat transfer in micropolar nanofluid over a vertical slender cylinder, Chin. Phy. Lett. 29 (12) (2012) 124701-5.

[35] Abdul Rehman, R. Bazai, S. Achakzai, S. Iqbal, M. Naseer, Boundary Layer Flow and Heat Transfer of Micropolar Fluid over a Vertical Exponentially Stretched Cylinder, App Comp Math, 4 (6) (2015) 424-430.

[36] O. D. Makinde, Thermal decomposition of unsteady non-Newtonian MHD Couette flow with variableProperties,. *Int. J. NumericalMethods for Heat & Fluid Flow, 25 (2) (2015) 252-264.*

[37] O. D. Makinde, Thermal analysis of a reactive generalized Couette flow of power law fluids between concentric cylindrical pipes, *European Physical Journal Plus, 129 (270) (2014) 1-9.*

[38] G. Singh, O. D. Makinde, Axisymmetric slip flow on a vertical cylinder with heat transfer. *Sains Malaysiana 43 (3) (2014) 483–489.*

[39] M. S. Tshehla, O. D. Makinde: Analysis of entropy generation in a variable viscosity fluid flow between two concentric pipes with a convective cooling at the surface. *Int. J. Phy. Sci.* 6 (25) (2011) 6053-6060.

[40] O. D. Makinde: Analysis of Non-Newtonian reactive flow in a cylindrical pipe. ASME - *Journal of Applied Mechanics 76 (2009) 1-5.*